Evaluation of Hofmeister Effects on the Kinetic Stability of Proteins

James M. Broering[†] and Andreas S. Bommarius*[,†,‡]

School of Chemical & Biomolecular Engineering, School of Chemistry and Biochemistry, and Parker H. Petit Institute for Bioengineering and Bioscience, Georgia Institute of Technology, 315 Ferst Drive, Atlanta, Georgia 30332-0363

Received: July 1, 2005; In Final Form: August 31, 2005

Dissolved salts are known to affect properties of proteins in solution including solubility and melting temperature, and the effects of dissolved salts can be ranked qualitatively by the Hofmeister series. We seek a quantitative model to predict the effects of salts in the Hofmeister series on the deactivation kinetics of enzymes. Such a model would allow for a better prediction of useful biocatalyst lifetimes or an improved estimation of protein-based pharmaceutical shelf life. Here we consider a number of salt properties that are proposed indicators of Hofmeister effects in the literature as a means for predicting salt effects on the deactivation of horse liver alcohol dehydrogenase (HL-ADH), α-chymotrypsin, and monomeric red fluorescent protein (mRFP). We find that surface tension increments are not accurate predictors of salt effects but find a common trend between observed deactivation constants and *B*-viscosity coefficients of the Jones−Dole equation, which are indicative of ion hydration. This trend suggests that deactivation constants (log $k_{d,obs}$) vary linearly with chaotropic *B*-viscosity coefficients but are relatively unchanged in kosmotropic solutions. The invariance with kosmotropic *B*-viscosity coefficients suggests the existence of a minimum deactivation constant for proteins. Differential scanning calorimetry is used to measure protein melting temperatures and thermodynamic parameters, which are used to calculate the intrinsic irreversible deactivation constant. We find that either the protein unfolding rate or the rate of intrinsic irreversible deactivation can control the observed deactivation rates.

Introduction and Background

As proteins in vivo as well as industrial biocatalysts usually operate in solutions containing moderate to high concentrations of different cosolutes, proteins are often exposed to conditions that impact their stability. Accurate predictions of cosolute effects on the protein can aid in formulation development for bioprocessing applications as well as in estimating useful biocatalyst lifetimes, protein-based pharmaceutical shelf life, or active protein lifetimes in vivo. Dissolved salts are one class of cosolute often found in bioprocessing media, often as buffer components or precipitating agents, but not all salts are equivalent at precipitating or stabilizing proteins. Well over a century ago, Hofmeister[1] found that, in addition to salt concentration, the nature of the dissolved salt determined the solubility of proteins in salt solutions. Hofmeister ranked salts on the basis of their effectiveness at salting-in or salting-out proteins in a series that now bears his name (Figure 1). Ions classified as chaotropes have a destabilizing effect on enzymes and aid in salting-in proteins in solution, whereas kosmotropes have a stabilizing effect on proteins and are effective salting-out agents. Chaotropes are often referred to as water structure breakers and kosmotropes are water structure makers; however, whether the ions impart a true water structure-breaking or -making effect on solution remains the subject of some debate.[2−5] Hofmeister ion effects become important at moderate to high salt concentrations (ionic strength > 0.01 mol/kg) beyond which the electrostatic shielding phenomenon described by the Debye−Hückel law is no longer accurate.[6] Furthermore, ion effects are generally additive, and anion effects tend to dominate solution behavior due to their asymmetric effect on polarizable water molecules.[7]

Despite its use to qualitatively explain trends of several protein properties in salt solutions, a useful *quantitative* description has not been developed which relates a salt's position in the Hofmeister series to its observed effect on any number of protein properties. Included in these are Hofmeister effects on enzyme deactivation kinetics. Cohn and Edsall showed that the salting out coefficients of salts, K_s, could be ranked according to the Hofmeister series:[8]

$$\log S = \log S_0 - K_s I \tag{1}$$

where S is the protein solubility in a salt solution with ionic strength I, and S_0 is the protein solubility in salt-free solution. Similarly, von Hippel and Wong showed that the melting temperature coefficients, K_m, could be ranked according to a salt's position in the Hofmeister series:[9]

$$T_m = T_{m0} - K_m c \tag{2}$$

where T_m is the melting temperature in a salt solution with concentration c and T_{m0} is the melting temperature in salt-free solution. Though these rankings are useful for estimating relative influences of different salts-on proteins, a quantitative model for Hofmeister effects would be even more powerful. Although our ultimate goal is the quantification and prediction of salt effects on the deactivation kinetics of proteins, in this initial study we aim to identify which of several proposed indicators of Hofmeister series position best correlates with salt effects

* Author to whom correspondance may be addressed. E-mail: andreas.bommarius@chbe.gatech.edu.
† School of Chemical & Biomolecular Engineering.
‡ School of Chemistry and Biochemistry.

10.1021/jp053618+ CCC: $30.25
Published on Web 10/07/2005

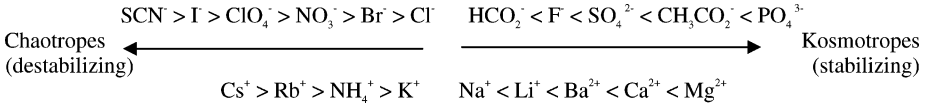

Figure 1. Hofmeister series.

on the deactivation kinetics of several unrelated model proteins. We will consider some of the most commonly offered indicators presently.

Influence of Surface Tension. Melander and Horvath attribute Hofmeister salt effects on proteins to the favorability of cavity formation for a cosolute ion in the protein solvation shell and demonstrate that a salt's surface tension increment σ can provide a quantitative measure of the salting-in and salting-out effects of electrolytes on proteins.[10] (The surface tension increment σ is defined from the equation $\gamma = \gamma_o + \sigma m$, where γ is the solution surface tension and m is the salt concentration.) They note that salts with large surface tension increments tend to salt-out proteins (i.e., are kosmotropes) and those with smaller surface tension increments will salt-in proteins. Others have found surface tension to be useful in describing some Hofmeister effects, but a number of exceptions are found which are not accounted for by surface tension arguments.[11−15] Despite these notable exceptions, surface tension increments still continue to be offered in the literature as predictors of ion effects on protein stability.[16]

Ion Hydration. Lavelle and Fresco show that the surface charge density of ions correlates well with the stability of nucleic acid triplexes and suggest that the same correlation would apply to protein stability.[17] Collins has also considered ion charge density to be important but has extended the idea to consider the increased ion hydration and water structure that result from increased charge density.[7,18−20] Small, high charge-density ions will bind water more tightly than larger, less charge-dense ions; thus, small, strongly hydrated ions are thought to be water structure formers (kosmotropes), and larger less hydrated ions are water structure breakers (chaotropes). The Jones−Dole equation relates these salt−solvent effects to the viscosity of the salt solution (η) relative to the viscosity of water (η_o):[21]

$$\eta/\eta_o = 1 + Ac^{0.5} + Bc + Dc^2 \qquad (3)$$

The term $Ac^{0.5}$ captures electrostatic (Debye−Hückel) effects and, at high salt concentrations (>0.1 M), becomes small relative to the ion−solvent interactions term characterized by the *B*-viscosity coefficient. The *D* term is only needed at very high salt concentrations. *B*-viscosity coefficients for several ions have been calculated and can be found in the literature,[22−25] and the numerical values rank ions in the order given by the Hofmeister series. Chaotropes have negative *B*-viscosity coefficients and kosmotropes have positive *B* values. Despite their plausible physical description of the solution environment and convenient ranking of Hofmeister ions, explicit relationships between *B*-viscosity coefficients and enzyme deactivation constants have not been explored, to the best of the authors' knowledge, prior to this work.

Excluded Volume. In addition to salt effects, several groups studying protein stability in solutions have considered the effects of a larger group of cosolutes including strong denaturants, such as urea, and stabilizing osmolytes, such as glycerol, trehalose, and other sugars. The simplest proposed explanations of cosolute effects claim that the excluded volume of the cosolute determines its effect on protein properties.[26−29] Excluded volume arguments hold that more energy is needed to create a cavity for the protein in a solution containing larger cosolutes. As a consequence, larger cosolutes in solution will stabilize protein structure by shifting the unfolding equilibrium to the more compact native state. Though consideration of excluded volume and molecular crowding can help explain cosolute stabilization of proteins,[30,31] they cannot account for the fact that some cosolutes destabilize proteins, so other explanations are needed to explain stabilizing as well as destabilizing effects of the entire range of cosolutes.

Preferential Interactions. Timasheff and co-workers have considered the stabilizing or denaturing effects to be due to preferential interaction of cosolutes with the protein surface.[15,32−35] Stabilizing cosolutes tend to be excluded from the protein-water surface, so the protein is stabilized by the resulting preferential hydration. Denaturants preferentially bind to the protein surface which destabilizes the native protein and causes the protein to unfold. Preferential binding or exclusion of cosolutes can be measured by equilibrium dialysis or vapor pressure osmometry[36,37] and is directly related to the difference in transfer energy between moving the native and unfolded protein from purely aqueous solution to solution containing cosolute.[32]

Transfer Model. The transfer model has been used to estimate transfer energies of both native and unfolded proteins.[38−40] To evaluate the total transfer energy for a protein, experimental data or models for the transfer energies of individual side chains or peptide backbone units are needed and can be found in the literature for select cosolutes.[8,39,41] Application of the transfer model requires structural information about the native and denatured states of the protein to be known, and though many native structures can be obtained from databases, the structures of unfolded protein must be modeled. Transfer energies for unfolded states can typically only be bounded using models which allow highly surface-accessible unfolded chains (upper bound) or more compact unfolded states (lower bound).[42] The lack of availability of either native state structures, component transfer energies for particular cosolutes, or accurate modeling for the denatured state can thus prohibit implementation of the transfer model in some cases. Baynes and Trout have eliminated the reliance on experimental individual group transfer energies by calculating preferential binding coefficients of glycerol and urea with native RNase A and RNase T1 directly from molecular dynamics simulations.[43] This does not, however, eliminate reliance on models to calculate transfer energies of the denatured state. Furthermore, the method cannot be applied if the native structure of the protein is unknown, as might be the case for a novel biocatalyst.

Focus of This Work. Though transfer energy models have been used to rigorously analyze the thermodynamic stability effects of a number of cosolutes, analyses tend to focus on one class of cosolute (e.g., only denaturants or stabilizers) or select extreme cases of each, for example urea and TMAO.[3] The salts of the Hofmeister series provide a middle ground for looking at a range of cosolute effects on a continuum, rather than just the extremes. However, a critical analysis of this middle ground is absent from the literature. Because anion effects tend to dominate,[7] we have analyzed the effects of a series of sodium salts covering the range of the Hofmeister series on the deactivation kinetics of three model proteins: horse liver alcohol dehydrogenase (HL-ADH), α-chymotrypsin, and monomeric red fluorescent protein (mRFP). As little knowledge exists about

TABLE 1: Experimental Molal Salt Concentrations (mol/kg) Giving Specified Water Activities[a]

salt	$a_w = 0.99$	$a_w = 0.97$	$a_w = 0.95$
NaI	0.298	0.865	1.390
$NaNO_3$	0.313	0.994	1.710
NaBr	0.301	0.890	1.445
NaCl	0.303	0.905	1.495
$NaHCO_2$	0.303	0.905	1.495
NaF	0.311	0.970	insol[b]
Na_2SO_4	0.255	0.865	1.530
$NaCH_3CO_2$	0.296	0.855	1.370

[a] Water activities were calculated using osmotic coefficients found in ref 44. [b] NaF is insoluble beyond ~1 *m*. The concentration−activity curve was extrapolated to reach a concentration where $a_w = 0.95$. A saturated solution containing 1.62 mol/kg (including insoluble salt) was used for deactivation experiments at this condition.

the importance Hofmeister effects on protein kinetic stability, we have focused on identifying which of the readily accessible proposed stability indicators (surface tension increments or *B*-viscosity coefficients) best predicts the ion effects on the protein deactivation.

Materials and Methods

Deactivation experiments were carried out in salt solutions with constant water activity, $a_w = 0.99$, 0.97, and 0.95. Salt concentrations giving these water activities were calculated from osmotic coefficients from the literature[44] and are listed in Table 1. HL-ADH and bovine α-chymotrypsin were obtained in lyophilized form from Sigma (A-9589, C-1429). Enzymes were dissolved in 50 mM HEPES buffer (pH 7.0) and mixed with buffered (50 mM HEPES pH 7.0) stock salt solutions to give enzyme−salt solutions with the desired water activity. Working protein concentrations in enzyme−salt solutions were measured via Bradford assay using Coomassie stain (Pierce, Rockford, IL) and were typically around 1 mg/mL for HL-ADH and 2.5 mg/mL for α-chymotrypsin. Enzyme−salt solutions were aliquotted into 0.65 mL thin-walled tubes and then placed into a water bath at the desired deactivation temperature. One tube of each solution was kept on ice to serve as an undeactivated ($t = 0$) sample. Tubes were periodically removed from the water bath and immediately placed in ice water to stop the deactivation reaction.

HL-ADH samples were centrifuged at 13000*g* for 2 min to collect precipitate which interferes with spectrophotometric readings. The supernatant (20 μL) was assayed for residual activity (relative to the undeactivated sample), v/v_o, by monitoring NADH production at 340 nm at 30 °C in 1 mL of 10 mM Tricine buffer (pH 9) containing 10 mM *n*-butanol (Aldrich 27,-067-9) and 0.8 mM NAD^+ (Sigma N-7129). First-order deactivation constants ($k_{1,obs}$) were then calculated from slopes of ln(residual activity) versus deactivation time ($\ln(v/v_o)$ vs t) plots. α-Chymotrypsin samples (10 μL) were assayed for residual activity at 30 °C using 4 mM *N*-benzoyl-L-tyrosine-*p*-nitroaniline (Sigma B-6760) as substrate in a 1 mL mixture of 50 mM Hepes buffer (pH 8) containing 30% (v/v) dimethylformamide (EMD DX1726-6). The reaction yields *p*-nitroaniline, which can be monitored spectrophotometrically at 410 nm. Active enzyme concentration (E) could then be calculated for each deactivation time and the slope of a plot of $1/E$ versus deactivation time (t) yielded the second-order deactivation coefficient, $k_{2,obs}$.

The mRFP gene was synthesized according to the sequence of Campbell and co-workers[45] and cloned into pProTet (BD Biosciences, San Jose, CA), which adds an N-terminal purification tag (MGHNHNHNHNHNGGDDDDKVVD-) to the expressed protein. Cultures were induced at OD 0.5 with 100 ng/mL anhydrotetracycline, and the overexpressed protein was purified with Talon metal affinity resin (Qiagen, Valencia, CA) 24 h after induction. The purified protein was dialyzed versus several changes of 50 mM HEPES pH 7.0 for at least 24 h to remove any salt and imidazole remaining from the purification steps. mRFP samples were mixed 1:1 with 2× concentrated stock−salt solutions to give 1× protein−salt solutions at the experimental water activities. Samples were aliquotted into 0.65 mL thin-walled tubes and incubated in a water bath at the desired deactivation temperature. Tubes were periodically removed and immediately placed in ice water to stop the deactivation reaction. Each sample (40 μL) was placed into wells of a 96-well plate, and the remaining fluorescence was measured using a FluoStar microplate reader (BMG LabTech, Offenburg, Germany) with $\lambda_{ex} = 544$ nm, $\lambda_{em} = 590$ nm. First-order deactivation constants ($k_{1,obs}$) were calculated from the slopes of plots of ln(residual fluorescence) versus deactivation time ($\ln(f/f_o)$ vs t).

Differential scanning calorimetry (DSC) was carried out using a NDSC-II (Calorimetry Sciences, Lindon, UT) on α-chymotrypsin and mRFP salt solutions with $a_w = 0.97$ using a scan rate of 1 °C/min. Scans were analyzed using CpCalc software available with the instrument.

Results

Deactivation Experiments. As a first test system, deactivation constants of HL-ADH were measured in a series of sodium salt solutions. The salt concentrations were chosen to keep the thermodynamic water activity within a set of salt solutions constant and sets where $a_w = 0.95$, 0.97, and 0.99 were used. Lower water activity indicates a less ideal solution (in the thermodynamic sense) due to increased salt content. HL-ADH deactivation was observed to follow first-order deactivation kinetics as shown in Figure 2A, consistent with previous reports.[46] To evaluate the proposed stability indicators, the logarithm of the observed deactivation constant, $\log k_{1,obs}$, was plotted versus the salt surface tension increment[10,16,47] and Jones−Dole *B*-viscosity coefficient[18] of the anion, as found in Figure 3. Values of each parameter for each ion can be found in Table 2.

According to the model by Melander and Horvath,[10] salts with high surface tension increments are typically expected to stabilize proteins, whereas those salts with less effect on surface tension are predicted to destabilize proteins. Figure 3A shows that this rationale does not hold for HL-ADH. As an example, the Hofmeister series ranks SO_4^{2-} and $CH_3CO_2^-$ as neighboring kosmotropes; thus, one would expect SO_4^{2-} and $CH_3CO_2^-$ to have similar stabilizing effects on protein stability. However, SO_4^{2-} has the largest surface tension increment and $CH_3CO_2^-$ has the smallest. If these ions' effects on protein stability were judged from their surface tension increments, one might expect them to have very different effects. These differences are not observed experimentally, though, as the measured deactivation constants can be ranked by the Hofmeister series, with SO_4^{2-} and $CH_3CO_2^-$ having similar effects on the protein. Clearly, the stabilizing effect of ions on HL-ADH cannot be predicted by surface tension increments.

Observed deactivation constants of HL-ADH, however, do show a trend with *B*-viscosity coefficients of the anions at all three water activities. The *B*-viscosity plot (Figure 3B) shows a distinct negative trend among the chaotropes ($B < 0$) with I^- being the most deactivating and Cl^- being the weakest, in agreement with the Hofmeister series. The slope of the chao-

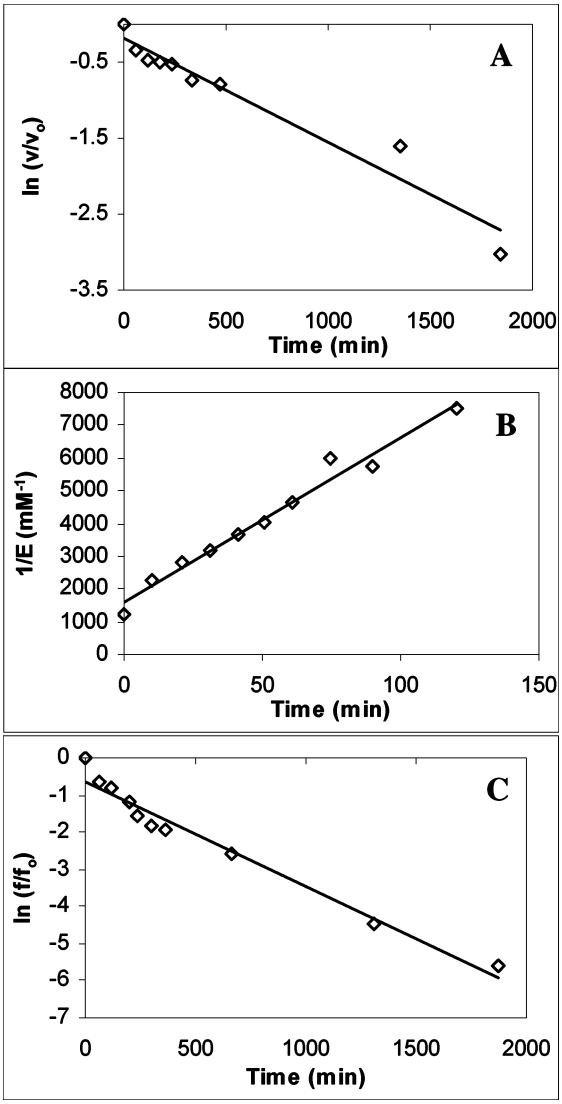

Figure 2. Deactivation kinetics of HL-ADH at 60 °C (A), α-chymotrypsin at 50 °C (B), and mRFP at 80 °C (C) in NaCl solutions with $a_w = 0.95$. A linear semilog plot of residual HL-ADH activity (v/v_o) with time demonstrates that HL-ADH deactivates via first-order kinetics. Second-order kinetics are observed for α-chymotrypsin deactivation, as evidenced by a linear trend in the plot of inverse of active enzyme concentration versus time. mRFP deactivation kinetics were determined to be first-order from the semilog plot of residual fluorescence (ln f/f_o) versus time.

tropic branch decreases with increasing water activity (i.e., lower salt content), which makes sense as the presence of less deactivating salt should translate into less change of deactivation of the enzyme. With the exception of sodium formate, much less difference is observed between deactivation constants measured in kosmotropic solutions despite the large differences in hydration of the anions as judged by their *B*-viscosity coefficients. We surmise that formate ion has a specific stabilizing interaction with HL-ADH that does not occur with other anions. Compared to the chaotropic portion of the curves, the kosmotropic branches appear relatively flat, suggesting that there is a minimum deactivation constant that could be attained. A similar dichotic trend with respect to chaotropes and kosmotropes is observed when deactivation constants are compared with surface charge density (data not shown).

To investigate whether our observed trends with *B*-viscosity coefficients were specific to HL-ADH, deactivation constants of α-chymotrypsin in the same series of salt solutions as HL-ADH were measured. Besides having different catalytic activity (cleavage of amide bonds), α-chymotrypsin is smaller than HL-ADH (25 kDa), is monomeric, and shares no common tertiary structure motifs with HL-ADH. Moreover, soluble α-chymotrypsin deactivates by a second-order mechanism due to degradation via autoproteolysis[48−50] as shown in Figure 2B. (There are some reports of chymotrypsin deactivating via first-order kinetics;[49,50] however, these observations were made with immobilized chymotrypsin samples and mass transfer limitations caused by the immobilization can lead to observed first-order deactivations, though the intrinsic deactivation rate may be of a different order.) Measured second-order deactivation constants, $k_{2,obs}$, for α-chymotrypsin in salt solutions at 50 °C were compared with *B*-viscosity coefficients, as with HL-ADH, and are shown in Figure 3E. Despite the different deactivation kinetics, a trend similar to that for HL-ADH was observed between the second-order deactivation constants and both *B*-viscosity coefficients and surface charge densities (not shown). Again, the deactivation effect of chaotropes decreased with increasing *B*-viscosity coefficient and surface charge density; however, the effect of kosmotropes on α-chymotrypsin deactivation is less marked. Chaotropic slopes again decreased with increasing water activity, and the kosmotropic branches of the curves still appear flat relative to the chaotropic branches, though there are some point-to-point variations.

To test the generalizability of these trends to a noncatalytic protein, we tested monomeric red fluorescent protein (mRFP). Though only slightly bigger than α-chymotrypsin (28.1 kDa), mRFP differs structurally from both α-chymotrypsin and HL-ADH. Because mRFP does not catalyze a reaction, it does not possess a chemically active site that must be folded correctly for the protein to function. However, the protein only fluoresces when folded properly so that the chromophore inside the β-barrel structure at the center of the protein is properly positioned.[45] Thus, mRFP fluorescence gives an indication of the amount of properly folded, active protein that exists, and mRFP fluorescence loss in salt solutions can be studied in the same way that enzyme deactivation was studied. mRFP was found to lose fluorescence according to first-order kinetics, as shown in Figure 2C. The first-order deactivation constants, $k_{1,obs}$, were again compared with *B*-viscosity coefficients, as shown in Figure 3F. A similar trend as with HL-ADH and α-chymotrypsin *B*-viscosity coefficients and the mRFP deactivation constants, $k_{1,obs}$, is observed. The trend with surface charge densities is also similar (not shown).

DSC Experiments. One of the simplest schemes for modeling irreversible enzyme deactivation is the Lumry−Eyring scenario:[51]

$$N \overset{K_u}{\longleftrightarrow} U \overset{k_1}{\longrightarrow} D \tag{4}$$

where native protein (N) reversibly unfolds to the unfolded state (U) which is then irreversibly converted to the deactivated state (D). In the classical Lumry−Eyring scenario, the U → D transition is defined as a first-order process; however, it is not difficult to envision other schemes where this transition follows other kinetics. Zale and Klibanov[52] have shown that the observed rate constant of the overall first-order N → D transition ($k_{1,obs}$) is related to the unfolding constant K_u ($K_u = [U]/[N]$) and first-order irreversible kinetic constants by

$$k_{1,obs} = \frac{k_1}{1 + 1/K_u} \tag{5}$$

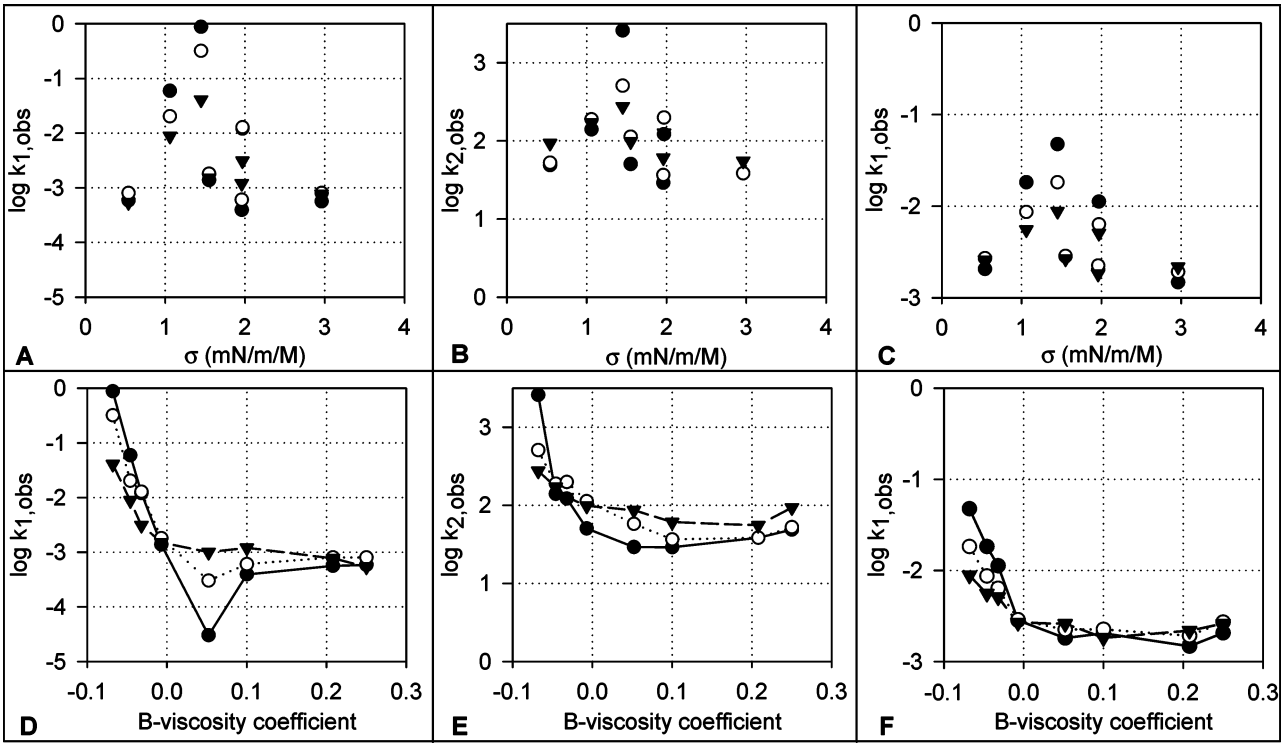

Figure 3. Evaluation of stability indicators with deactivation constants of HL-ADH at 60 °C (A, D), α-chymotrypsin at 50 °C (B, E), and mRFP at 80 °C (C, F). All deactivations occurred at pH 7.0. Deactivation constants were measured in salt solutions with water activities of $a_w = 0.95$ (●), 0.97 (○), and 0.99 (▼). (A−C) no correlation is observed with surface tension increments for any of the proteins tested. (D−F) Correlation with *B*-viscosity coefficients. Deactivation constants appear to vary linearly with chaotropic *B*-viscosity coefficient ($B < 0$) but are relatively unaffected by kosmotropic salts ($B > 0$).

TABLE 2: Hofmeister Ion Property Comparison[a]

source	B (M^{-1}) ref 18	σ [(mN/m)/M] ref 53	ref 10	ref 47
I^-	−0.068	**1.45**	1.02	1.23
NO_3^-	−0.046		**1.06**	
Br^-	−0.032	**1.97**	1.32	1.83
Cl^-	−0.007	**1.55**	1.64	2.08
HCO_2^-	0.052			
F^-	0.100			**1.83**
SO_4^{2-}	0.208	**2.96**	2.73	2.90
$CH_3CO_2^-$	0.250	**0.54**		0.93

[a] Surface tension increments listed are for the sodium salt of the ion indicated. To achieve the most complete listing of values, several overlapping data sets from the literature were combined. Bold values indicate those used to plot data in Figure 3. The conclusion that surface tension increments do not correctly rank Hofmeister ions is unchanged regardless of which combination of data is used, largely due to the low value for acetate seen in both ref 53 and ref 47.

By similar reasoning, it can be shown that for a second-order irreversible step, as in the case with α-chymotrypsin, the observed deactivation constant is given by

$$k_{2,obs} = k_2\left(\frac{1/K_u}{1 + 1/K_u}\right)^2 \tag{6}$$

For either case, if any two of the parameters, k_{obs}, K_u, or k, are known, the third can be calculated, and the individual contributions of unfolding and irreversible denaturation to the observed kinetics can be evaluated using eq 5 or 6. The derivation of eq 6 can be found in the Supporting Information.

Differential scanning calorimetry (DSC) can be used to measure the melting temperature (T_m) and enthalpy of unfolding (ΔH_u) and heat capacity change (ΔC_p) for the N → D transition. The melting temperature is the temperature where 50% of the protein is unfolded or [N] = [D] and a measure of the protein's thermodynamic stability. With T_m, ΔH_u and ΔC_p known, the unfolding constant at any temperature T can be calculated with

$$K_u(T) = \exp\left\{-\frac{\Delta H_u}{RT}\left(1 - \frac{T}{T_m}\right) - \frac{\Delta C_p}{RT}\left[T - T_m - T\ln\left(\frac{T}{T_m}\right)\right]\right\} \tag{7}$$

Melting temperatures and unfolding enthalpies of salt solutions with $a_w = 0.97$ containing α-chymotrypsin or mRFP were measured with DSC and used in eq 7 to calculate the unfolding constant at the temperatures where the previous deactivation experiments were performed ($T = 50$ °C for α-chymotrypsin, $T = 80$ °C for mRFP). With calculated unfolding and overall kinetic constants, the intrinsic irreversible kinetic constants, k_1 or k_2, could then be calculated from eq 5 (for mRFP) or 6 (for α-chymotrypsin). The calculated irreversible deactivation constants were compared to the observed deactivation constants ($k/k_{d,obs}$) to determine their contribution to the overall kinetics. The measured DSC data and calculated constants can be found in Table 3.

DSC was attempted with HL-ADH as well; however, HL-ADH samples aggregate significantly during DSC, and T_m and ΔH could not be determined. mRFP samples exhibited two transitions during DSC. The first transition occurs between 72 and 85 °C, and the second transition is seen between 87 and 96 °C, depending on the salt solution sampled. The double transition is due to the presence of another 21 kDa protein in the mRFP samples that could not be removed during purification. The DSC peaks of the mRFP samples are usually well separated, so we are confident that our reported melting temperatures and unfolding enthalpies for mRFP are accurate for the protein and not severely influenced by the presence of the impurity. This impurity was also noted by Campbell[45] and

TABLE 3. Melting Temperature and Kinetic Parameter Comparison

α-Chymotrypsin Thermodynamic Parameters at $T = 50$ °C							
salt	T_m (°C)	ΔH (kJ/mol)	ΔC_p [kJ/(mol K)]	K_u	$k_{2,obs}$ $(mM\ s)^{-1}$	k_2 $(mM\ s)^{-1}$	$k/k_{d,obs}$
I^-	43.6	357	3.03	7.89	8.456	668	79.0
NO_3^-	49.3	364	0.35	1.25	3.142	16.0	5.1
Br^-	50.9	523	5.70	0.77	3.300	10.3	3.1
Cl^-	54.1	454	2.79	0.31	1.883	3.2	1.7
HCO_2^-	55.7	425	0.99	0.19	0.960	1.4	1.4
F^-	58.3	462	2.50	0.09	0.610	0.731	1.2
SO_4^{2-}	59.6	396	1.97	0.07	0.638	0.724	1.1
$CH_3CO_2^-$	55.1	472	2.84	0.23	0.872	1.32	1.5
mRFP Thermodynamic Parameters at $T = 80$ °C							
salt	T_m (°C)	ΔH (kJ/mol)	ΔC_p [kJ/(mol K)]	K_u	$k_{1,obs}$ (s^{-1})	k_1 (s^{-1})	$k/k_{d,obs}$
I^-	89.0	101	−4.94	0.091	3.04×10^{-4}	3.65×10^{-3}	12.0
NO_3^-	90.3	105	−1.15	0.074	1.44×10^{-4}	2.09×10^{-3}	14.5
Br^-	90.2	110	1.64	0.087	1.05×10^{-4}	1.31×10^{-3}	12.5
Cl^-	91.7	119	0.11	0.057	4.78×10^{-5}	8.80×10^{-4}	18.4
HCO_2^-	92.4	136	1.53	0.054	3.72×10^{-5}	7.32×10^{-4}	19.6
F^-	92.6	136	2.92	0.057	3.74×10^{-5}	6.95×10^{-4}	18.6
SO_4^{2-}	93.8	153	−1.20	0.031	3.19×10^{-5}	1.07×10^{-3}	33.5
$CH_3CO_2^-$	94.7	100	−13.35	0.007	4.50×10^{-5}	6.23×10^{-3}	138.5

colleagues, who hypothesized that it is a cleaveage fragment of mRFP. If this is the case, one would expect that the larger, complete mRFP would have a higher T_m than a truncated fragment, so we attribute the second peak to the native form of mRFP. As a native PAGE gel of mRFP samples shows a red band of mRFP at 28 kDa and no fluorescence or visible color is observed at 21 kDa, we conclude that all fluorescence of our mRFP samples is due to native state 28 kDa protein and not the 21 kDa impurity.

The measured melting temperatures of α-chymotrypsin and mRFP (including those measured for the 21 kDa impurity, T_{m1}) were compared with *B*-viscosity coefficients, as shown in Figure 4. The melting temperatures for α-chymotrypsin and the mRFP impurity show a similar trend with *B*-viscosity coefficients as with the measured deactivation constants (though the slopes of the chaotropic portions are reversed due to the opposite sign of (log $k_{d,obs}$) and T_m): T_m varies linearly with *B*-viscosity coefficients in chaotropic solutions ($B < 0$) and is less influenced by kosmotropic solutions ($B > 0$). The melting temperatures for native mRFP (T_{m2}) also show linear variation with chaotropic *B*-viscosity coefficients but also continue to increase beyond $B > 0$.

Examination of the calculated unfolding and irreversible deactivation constants, K_u and $k_{i,obs}$, shows that for α-chymotrypsin in kosmotropic and weakly chaotropic (NaCl) solutions, the ratios of the irreversible intrinsic rate constant to the observed deactivation constant $k_2/k_{2,obs}$ are near unity, suggesting that the observed deactivation rate is controlled by the intrinsic irreversible deactivation rate. Though both K_u and k_2 increase as solutions become more chaotropic, K_u increases more, such that, with the strongest chaotrope solution (NaI), the intrinsic irreversible rate is much faster than the observed reaction rate, indicating that the deactivation rate is now limited by the rate of protein unfolding. In contrast, analysis of mRFP constants shows intrinsic rate constants k_1 of 1−2 orders of magnitude higher than observed rate constants $k_{1,obs}$ in all salt solutions, indicating that the overall deactivation is controlled by the unfolding of the protein in all of the investigated salt solutions.

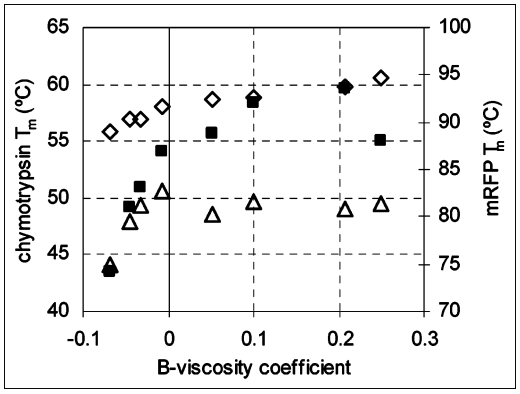

Figure 4. Comparison of α-chymotrypsin melting temperatures (■) and mRFP melting temperatures T_{m1} (△) and T_{m2} (◇) measured in salt solutions with $a_w = 0.97$ with *B*-viscosity coefficients.

Discussion

Though explanations that attribute cosolute effects on protein stability to the excluded volume of the cosolutes and molecular crowding effects can account for the stabilizing effects of a number of cosolutes, these explanations cannot account for the occurrence of cosolute-induced destabilization. As a result, attention in the literature has focused on other properties that may be useful predictors of a cosolute's effect on protein stability. To predict the effects of dissolved salts on proteins, both *B*-viscosity coefficients and salt surface tension increments have been suggested as possible indicators of a salt's Hofmeister effect. Despite reports that surface tension increments are incomplete predictors of protein stability,[13−15,32] surface tension increments continue to be offered as explanations for and predictors of Hofmeister effects.[16] Our protein deactivation data conclusively demonstrate that surface tension increments do not predict effects of salts in the order of the Hofmeister series. For example, surface tension increments would predict the stabilizing kosmotrope F^- and the moderate chaotrope Br^- to have similar effects on protein stability because they have similar surface tension increments. The experimental rate constants measured here tend to follow the order predicted by the Hofmeister series and thereby reinforce the point that surface tension increments cannot predict the effects of ions on protein stability.

TABLE 4: Comparison of Model Protein Characteristics

	HL-ADH	α-chymotrypsin	mRFP
subunit size (AA)	374	245	225
quaternary structure	dimer	monomer	monomer
MW (kDa)	80	25	28[a]
pI	8.31	8.52	5.65
deactivation order	1st	2nd	1st

[a] mRFP molecular weight includes the weight of the 225 amino acid monomer (25.4 kDa) and the weight of the 25 amino acid purification tag (2.7 kDa).

Similar trends between the log of our experimentally measured deactivation constants (log $k_{d,obs}$) and *B*-viscosity coefficients are observed for all three of the proteins tested. Several properties of these proteins are compared in Table 4. The size, multimericity, and deactivation kinetics of the proteins do not appear to influence this trend. The isoelectric points of the model proteins also fall on both sides of the experimental pH (7.0), indicating that the surface charge of the protein does not affect our observed trend.

Among deactivation constants observed in chaotropic solutions, the k_{obs} for each salt is distinct from the others and the constants decrease in the order predicted by the Hofmeister series ($I^- > NO_3^- > Br^- > Cl^-$). With respect to both *B*-viscosity coefficients and anion surface charge densities, the trend between log k_{obs} and either stability indicator appears to be linear in chaotropic solutions. The fact that this linear trend is observed among all of our model proteins suggests that it may be exploited to predict changes in deactivation constants of other proteins from one chaotropic salt solution to another.

Because it appears that less hydration on chaotropic ions leads to accelerated protein deactivation, one might expect that more ion hydration would lead to protein stabilization and impede protein deactivation. If this were the case, one would expect to observe lower deactivation constants in salt solutions with larger *B*-viscosity coefficients. However, this is not what is observed experimentally. Rather than observing decreasing deactivation constants with increasing *B*-viscosity coefficients, we see little difference between deactivation constants in kosmotropic solutions, and even a ranking that could hold for all three proteins (e.g., least stabilizing salt to most stabilizing salt) is not immediately clear. The fact that the kosmotropic portion of the log $k_{d,obs}$ versus *B*-viscosity coefficient plots is relatively flat suggests that there may be a limiting, asymptotic value of $k_{d,obs}$ for the kinetic protein deactivation in salt solutions. Kosmotropic salts, it would appear, cannot slow protein deactivation past a certain point—they only prevent it from occurring faster. We are currently investigating whether other well-known stabilizers (e.g., glycerol and TMAO) can achieve slower deactivation rates or whether they are subject to the same apparent minimum.

Though ion hydration clearly affects protein deactivation rates measured in chaotropic solutions, it is somewhat puzzling why deactivation rates in kosmotropic solutions seem to be independent of ion hydration. We hypothesize that preferential interaction/exclusion phenomena, observed by Timasheff and co-workers, might be able to explain this difference. If chaotropic salts are preferentially bound to the protein−water interface like other destabilizing cosolutes, then the differences in hydration of the various chaotropic ions lead to a proportional effect on the protein stability by lessening the hydrophobic effect at the protein−solution interface. Conversely, if kosmotropic salts are preferentially excluded from the protein−solution interface, then the protein "sees" less of the kosmotropic ions in solution and reacts less to the differences in hydration among the kosmotropic ions, because the protein itself is already strongly hydrated. As a result, kosmotropes would appear to have similar effects on the protein, consistent with our observed results.

Thermal unfolding parameters were measured with DSC in an attempt to discern whether our observed deactivation rates were limited by protein unfolding (N → U) or the rate of the irreversible transition from the unfolded to the denatured state (U → D). The magnitudes of the relative deactivation rates ($k/k_{d,obs}$) show different controlling mechanisms, depending on the protein and the salt environment. mRFP deactivation seems to be limited by protein unfolding in all solutions. Though deactivation of α-chymotrypsin appears to be controlled by the irreversible transition in kosmotropic solutions, unfolding appears to become more limiting with increasing chaotropicity and was found to control observed deactivation in strongly chaotropic media. Given that both modes of control are observed with our model proteins, generalizations as to the controlling step of observed deactivation cannot be made. In light of this finding, the observed similarities of protein deactivation as a function of ion hydration among the three proteins studied are all the more remarkable.

Conclusions

In summary, the lack of correlation between observed deactivation constants and surface tension reinforces earlier reports that surface tension increments are not good predictors of ion effects on proteins. The strong linear correlation between chaotropic deactivation constants and *B*-viscosity coefficients for our model proteins suggests a generalizable phenomenon which is useful to predict changes in protein deactivation rate constants in chaotropic solutions. Furthermore, deactivation rates measured in kosmotropic solutions appear to be independent of ion hydration and suggest that a minimum deactivation rate may exist for each protein in salt solutions. We hypothesize that preferential binding and exclusion of salts from the protein−solution interface may explain our observed variation in $k_{d,obs}$ with chaotropic and kosmotropic *B*-viscosity coefficients, and we are currently attempting to experimentally confirm preferential binding and exclusion of our salts with our model proteins to validate this hypothesis. Measurements of protein melting temperatures in salt solutions with DSC and evaluation of relative deactivation rates suggest that our observed kinetic deactivation constants can be limited by either protein unfolding or the irreversible transformation rate. Despite these different controlling mechanisms, the same deactivation trends with *B*-viscosity coefficients are still observed with three very different model proteins. This common trend, especially in chaotropic solutions, could be used to predict kinetic deactivation rates and impact protocols to accelerate medical diagnostics and testing of protein-based pharmaceutical shelf lives or industrial biocatalyst lifetimes.

Acknowledgment. We thank Sean Holton, who measured some of the HL-ADH and α-chymotrypsin deactivation constants, Bernard Loo for providing the mRFP construct for expression and evaluation, and Tien Le for measuring some of the mRFP deactivation kinetics. We also thank Dr. Loren Williams for the use of DSC instrumentation. J.M.B. is supported by a National Science Foundation Graduate Research Fellowship.

Supporting Information Available: The derivation of second-order observed deactivation constant is available free of charge via the Internet at http://pubs.acs.org.

References and Notes

(1) Hofmeister, F. *Arch. Exp. Pathol. Pharmakol.* **1888**, *24*, 247.
(2) Hribar, B.; Southall, N. T.; Vlacy, V.; Dill, K. A. *J. Am. Chem. Soc.* **2002**, *124*, 12302.
(3) Zou, Q.; Bennion, B. J.; Daggett, V.; Murphy, K. P. *J. Am. Chem. Soc.* **2002**, *124*, 1192.
(4) Batchelor, J. D.; Olteanu, A.; Tripathy, A.; Pielak, G. J. *J. Am. Chem.* Soc. **2004**, *126*, 1958.
(5) Omta, A. W.; Kropman, M. F.; Woutersen, S.; Bakker, H. J. *Science* **2003**, *301*, 347.
(6) Prausnitz, J. M.; Lichtenthaler, R. N.; Azevedo, E. G. d. *Molecular Thermodynamics of Fluid-Phase Equilibria*, 3rd ed.; Prentice-Hall: Upper Saddle River, NJ, 1999.
(7) Collins, K. D.; Washabaugh, M. W. *Q. Rev. Biophys.* **1985**, *18*, 323.
(8) Cohn, E. J.; Edsall, J. T. *Proteins, Amino Acids, and Peptides*; Reinhold: New York, 1943.
(9) von Hippel, P. H.; Wong, K. Y. *Science* **1964**, *145*, 577.
(10) Melander, W.; Horvath, C. *Arch. Biochem. Biophys.* **1977**, *183*, 200.
(11) Arakawa, T.; Bhat, R.; Timasheff, S. N. *Biochemistry* **1990**, *29*, 1914.
(12) Arakawa, T.; Timasheff, S. N. *Methods Enzymol.* **2003**, *114*, 49.
(13) Cioci, F. *J. Phys. Chem.* **1996**, *100*, 17400.
(14) Cioci, F. *AIChE J.* **1997**, *43*, 525.
(15) Lin, T. Y.; Timasheff, S. N. *Protein Sci.* **1996**, *5*, 372.
(16) Maheshwari, R.; Sreeram, K. J.; Dhathathreyan, A. *Chem. Phys. Lett.* **2003**, *375*, 157.
(17) Lavelle, L.; Fresco, J. R. *Biophys. Chem.* **2003**, *105*, 681.
(18) Collins, K. D. *Biophys. J.* **1997**, *72*, 65.
(19) Collins, K. D. *Proc. Natl. Acad. Sci. U.S.A.* **1995**, *92*, 5553.
(20) Kiriukhin, M. Y.; Collins, K. D. *Biophys. Chem.* **2002**, *99*, 155.
(21) Jones, G.; Dole, M. *J. Am. Chem. Soc.* **1929**, *51*, 2950.
(22) Krestov, G. *Thermodynamics of Solvation: Solutions and Dissolution, Ions and Solvents, Structure and Energetics*; Horwood: New York, 1991.
(23) Kaminsky, M. *Discuss. Faraday Soc.* **1957**, *24*, 171.
(24) Robinson, J. B., Jr.; Strottmann, J. M.; Stellwagen, E. *Proc. Natl. Acad. Sci. U.S.A.* **1981**, *78*, 2287.
(25) Jenkins, H. D. B. *Chem. Rev.* **1995**, *95*, 2695.
(26) Patel, C. N.; Noble, S. M.; Weatherly, G. T.; Tripathy, A.; Winzor, D. J.; Pielak, G. J. *Protein Sci.* **2002**, *11*, 997.
(27) Cheung, M. S.; Klimov, D.; Thirumalai, D. *Proc. Natl. Acad. Sci. U.S.*A. **2005**, *102*, 4753.
(28) Winzor, D. J.; Wills, P. R. *Biophys. Chem.* **1986**, *25*, 243.
(29) Minton, A. P. Molecular Crowding: Analysis of Effects of High Concentrations of Inert Cosolutes on Biochemical Equilibria and Rates in terms of Volume Exclusion. In *Energetics of Biological Macromolecules, Part B*; Ackers, G., Johnson, M., Eds.; Academic: San Diego, CA, 1998; Vol. 295, p 127.
(30) Hall, D.; Minton, A. P. *Biochim. Biophys. Acta* **2003**, *1649*, 127.
(31) O'Connor, T. F.; Debenedetti, P. G.; Carbeck, J. D. *J. Am. Chem.* Soc. **2004**, *126*, 11794.
(32) Arakawa, T.; Timasheff, S. N. *Biochemistry* **1982**, *21*, 6545.
(33) Arakawa, T.; Bhat, R.; Timasheff, S. N. *Biochemistry* **1990**, *29*, 1914.
(34) Timasheff, S. N. *Biochemistry* **1992**, *31*, 9857.
(35) Timasheff, S. N. *Biochemistry* **2002**, *41*, 13473.
(36) Lee, J. C.; Timasheff, S. N. *Biochemistry* **1974**, *13*, 257.
(37) Courtenay, E. S.; Capp, M. W.; Anderson, C. F.; Record, M. T. *Biochemistry* **2000**, *39*, 4455.
(38) Nozaki, Y.; Tanford, C. *J. Biol. Chem.* **1970**, *245*, 1648.
(39) Bolen, D. W. Protein Stabilization by Naturally Occurring Osmolytes. In *Protein Structure, Stability, and Folding*; Murphy, K. P., Ed.; Humana Press: Totowa, NJ, 2001; Vol. 168, p 17.
(40) Auton, M.; Bolen, D. W. *Biochemistry* **2004**, *43*, 1329.
(41) Nozaki, Y.; Tanford, C. *J. Biol. Chem.* **1963**, *238*, 4074.
(42) Creamer, T. P.; Srinsivasan, R.; Rose, G. D. *Biochemistry* **1997**, *36*, 2832.
(43) Baynes, B. M.; Trout, B. L. *J. Phys. Chem. B* **2003**, *107*, 14058.
(44) Lobo, V. M. M. *Handbook of Electrolyte Solutions*; Elsevier: Oxford, England, 1989; Vol. B.
(45) Campbell, R. E.; Tour, O.; Palmer, A. E.; Steinbach, P. A.; Baird, J. S.; Zachary, D. A.; Tsien, R. Y. *Proc. Natl. Acad. Sci. U.S.A.* **2002**, *99*, 7877.
(46) Higgins, A. C.; Johnson, D. B. *Int. J. Biochem.* **1977**, *8*, 807.
(47) Weissenborn, P. K.; Pugh, R. J. *J. Colloid Interface Sci.* **1996**, *184*, 550.
(48) Kumar, S.; Hein, G. E. *Biochemistry* **1970**, *9*, 291.
(49) Kawamura, Y.; Nakanishi, K.; Matsuno, R.; Kamikubo, T. *Biotechnol. Bioeng.* **1981**, *23*, 1291.
(50) Kim, J.; Grate, J. W. *Nano Lett.* **2003**, *3*, 1219.
(51) Lumry, R.; Eyring, H. *J. Phys. Chem.* **1954**, *58*, 110.
(52) Zale, S. E.; Klibanov, A. M. *Biotechnol. Bioeng.* **1983**, *25*, 2221.
(53) Abramzon, A. A.; Gaukhberg, R. D. *Russ. J. Appl. Chem.* **1993**, *66*, 1139; continued in **1993,** 66 (7), 1315 and 66 (8), 1473.